Impact of DG Interface Control on Islanding Detection and Nondetection Zones

H. H. Zeineldin, *Member, IEEE*, Ehab F. El-Saadany, *Senior Member, IEEE*, and M. M. A. Salama, *Fellow, IEEE*

***Abstract*—Islanding detection of Distributed Generation (DG) is considered as one of the most important aspects when interconnecting DGs to the distribution system. With the increasing penetration and reliance of the distribution systems on DGs, new interface control strategies are being proposed. Aside from its main task of supplying active power, the DG could provide voltage support, improve the power factor, or mitigate other power quality problems. This paper examines the impact of the interface control strategy of inverter based DGs on islanding detection. The Nondetective Zone (NDZ) for over/under voltage and over/under frequency is derived analytically for each interface control and validated by simulation.**

***Index Terms*—Distributed generation (DG), interface control, inverter, islanding, pulse-width modulation.**

I. Introduction

DISTRIBUTED generation (DG) provides many potential benefits, such as peak shaving, fuel switching, improved power quality and reliability, increased efficiency, and improved environmental performance. Many countries are trying to meet the targets set in the Kyoto Protocol to reduce greenhouse gas emissions. DG provides an attractive option to accomplish this task. In the last few years, small DGs in the range of 100 kW have gained popularity amongst industry and utilities.

For DG systems producing a DC voltage, an inverter is used to interface the DG system with the grid. The switching of the inverter is determined based on a certain implemented control strategy [1]. The DG could be designed to supply active power or both active and reactive power. Aside from controlling the DG output power, the DG interface control performs an additional function, which is anti-islanding protection [2]. A DG is islanded when it supplies power to some loads while the main utility source is disconnected.

Anti-islanding detection methods can be divided into two main groups: passive and active methods. In passive methods, the decision whether an islanding condition occurred or not is based on measuring a certain system parameter and comparing it with a predetermined threshold. Active methods are designed to force the DG to be unstable during an islanding situation.

Most of the islanding detection methods developed focused on DGs that operate at unity power factor. Recently, much work has been focusing on the DG interface to the grid and its operation and control. In [3], the interface control was designed to supply active power and improve the power factor at the point of interconnection of the DG. In [4], the proposed interface control takes into account DG islanding protection by proposing a control scheme that supplies active power, improves power factor and provides active islanding detection. In [5], a new control scheme for DGs using a current controlled Voltage Source Inverter (VSI) was proposed. Besides conditioning the power fed by the DG, power quality problems were mitigated. In [6], the interface control was designed to provide voltage support by supplying both active and reactive power, especially during the peak load time. The mitigation of unbalance in voltage and harmonics using the interface control of the DG was proposed in [7]. In [8] and [9], control techniques of inverter based DGs that focus on improving the power quality and ensuring continuity of supply were discussed. With distribution systems increasing reliance on DGs, utilizing the DG to inject reactive power aside from supplying active power is one of the targets in the DG interface design.

In this paper, several interface controls for DGs are presented and their performance is studied during an islanding situation. Based on the performance of the interface control, an additional parameter is implemented in parallel with the Over/Under Voltage and Over/Under frequency (OVP/UVP and OFP/UFP) for some of the presented interfaces to reduce the NDZ. The impact of DG interface control on the NDZ of OVP/UVP and OFP/UFP is analyzed.

The paper is organized as follows: Section II presents an overview on different anti-islanding protection methods. Simulation results illustrating the performance of each interface control during an islanding condition is presented in Section III. The effect of the interface control on the NDZ of OVP/UVP and OFP/UFP is discussed in Section IV. In Section V, the scope of the paper is discussed. Finally, conclusions are drawn in Section V.

II. DG Islanding Protection

DG systems are connected to the distribution system through an inverter as shown in Fig. 1. The inverter performs two main functions:

1) Controlling the active power output of the DG and, in some cases, injecting a suitable amount of reactive power to mitigate a power quality problem.
2) According to the IEEE Standard 1547, the DG should be equipped with an anti-islanding detection algorithm, which could be performed using the inverter interface control (active methods).

Manuscript received February 17, 2005; revised May 13, 2005. Paper no. TPWRD-00091-2005.

The authors are with the Department of Electrical and Computer Engineering, University of Waterloo, Waterloo, ON N2L 3G1, Canada (e-mail: hhmzeine@engmail.uwaterloo.ca).

Digital Object Identifier 10.1109/TPWRD.2005.858773

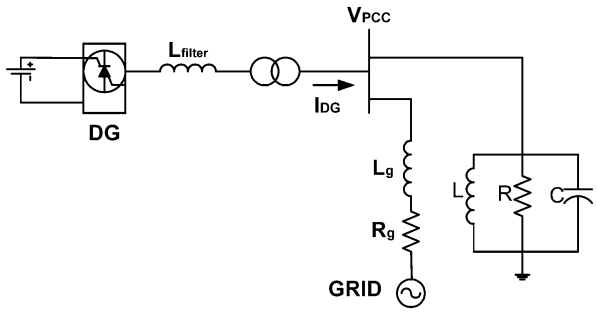

Fig. 1. Single line diagram of the system under study consisting of a DG, grid and RLC load.

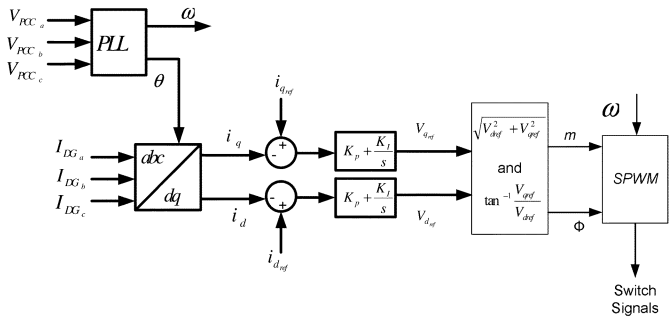

Fig. 2. Block diagram of a constant current controlled inverter.

As mentioned earlier, passive islanding detection techniques depend on measuring system parameters and setting thresholds for the measurable parameters. The main challenge when designing a passive islanding detection method is the choice of a suitable islanding measure and its threshold value. Thresholds are chosen such that the islanding detection algorithm will not operate for other disturbances on the system. As a result, passive methods suffer from large NDZ.

Over/under voltage and frequency is one of the simplest passive methods used in islanding detection. The thresholds on the voltage and frequency and the maximum allowable islanding detection trip time could be found in [2], [10]. Unfortunately, if the load and the generation on the island are closely matched, the change in voltage and frequency might be very small and within the thresholds, thus leading to an undetected islanding situation.

Parameters used to detect islanding include Total Harmonic Distortion (THD), the rate of change of active power, the ratio of frequency variation to load variation [11]–[13]. Other parameters used for passive islanding detection methods can be found in [14]. To enhance the performance of islanding detection methods and decrease the NDZ, several methods have been proposed which use more than one parameter to detect islanding. In [15], both the rate of change of voltage and change in power factor were used to detect islanding. In [16], islanding was detected using the voltage unbalance and the THD of the DG current. In [17], both reactive and active power variations were used as means for islanding detection.

In active methods, small variations at the output of the DG are created by designing a control circuit that provides the necessary variations. If the DG is operating in parallel to the distribution system, negligible changes occuring in the frequency or output power will not be sufficient in initiating the operation of the protective relay responsible for disconnecting the DG. However, once the utility is disconnected, the variation becomes significant and the DG is disconnected. Unfortunately, the small changes produced by the active methods' control circuit may affect the power quality of the system. Active methods include Active Frequency Drift method (AFD), output power variation, Slip Mode Frequency Shift, and etc. [14].

Section III studies the performance of each interface control during an islanding condition. Active power, reactive power, frequency and voltage waveforms are monitored. Based on the simulation results, an additional parameter is implemented in parallel with the OVP/UVP and OFP/UFP to decrease the NDZ.

III. DG Performance During an Islanding Condition

The system under study consists of a 100 kW inverter based DG connected to an RLC load having a quality factor of 1.8 and a grid as illustrated in Fig. 1. The filter inductance is dependent on the maximum switching frequency and the inverter DC voltage [5], [18]. The system, controller, and load parameters are given in the Appendix [19]. The performance of the DG under normal and islanded operating conditions was studied and simulated on PSCAD/EMTDC. Based on [10], the real load power was adjusted to place the inverter at 25%, 50%, 100%, and 125% of the inverter's rated output. The reactive power was adjusted between 95% and 105% of the balanced condition (unity power factor loading) in 1% steps [10]. For brevity, the following four loading conditions are presented:

- Case 1) Load is adjusted to operate the inverter at 100% of its rated active power output and 100% reactive power balance.
- Case 2) Load is adjusted to operate the inverter at 50% of its rated active power output and 100% reactive power balance.
- Case 3) Load is adjusted to operate the inverter at 100% of its rated active power output and 101% of the reactive power balance condition.
- Case 4) Load is adjusted to operate the inverter at 125% of its rated active power output and 95% of the reactive power balance condition.

A. *Constant Current Controlled Inverter*

The DG interface control is designed to supply constant current output as shown in Fig. 2. For this interface control, both I_d and I_q components of the DG output current are controlled to be equal to a preset value (I_{dref} and I_{qref}). To examine the performance of the DG under islanding conditions, the grid was disconnected at $t = 3$ seconds. Figs. 3–6 present the active power output of the DG, reactive power output of the DG, frequency and voltage at the PCC. The DG was operated at unity power factor by setting I_{qref} to zero.

Based on the simulation results, there are cases (Case 2 and Case 4) where the OVP/UVP and OFP/UFP will be capable of detecting islanding and others (Case 1 and Case 3) where it would fail. The significant feature of this interface control is that both the voltage and DG active power output decrease during an islanding situation and one of them could be used as a measure to detect islanding. This is as a result of the constant current operation of the DG. For a constant preset current output

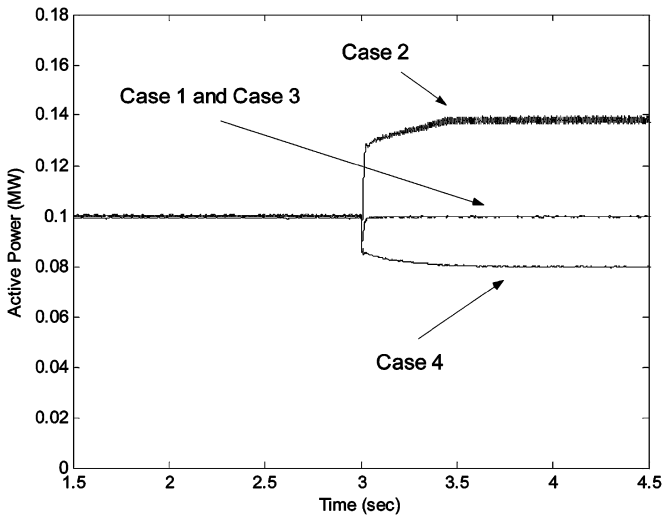

Fig. 3. Active power output of the DG.

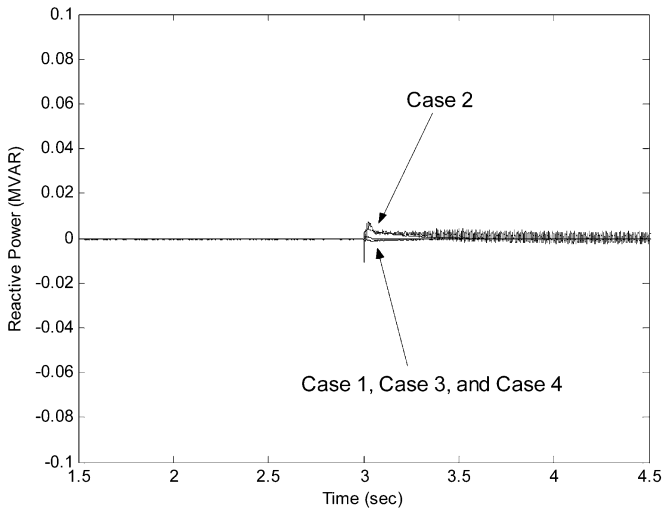

Fig. 4. Reactive power output of the DG.

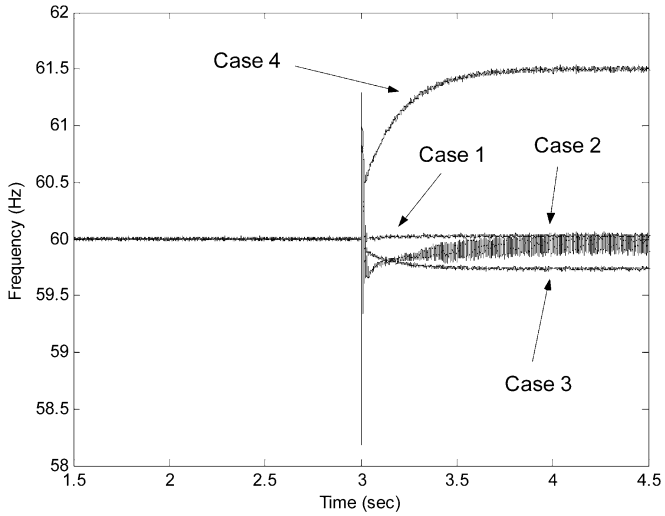

Fig. 5. Frequency at the PCC.

and fixed load impedance, once islanding occurs, the voltage and DG active power become dependent on the value of load impedance. In other words, for a 100 kW DG operating at a line voltage of 480 V, the load resistance value, for which a negligible change will occur in both voltage and active power, is 2.304 Ω. With the utility connected, the DG active power output is maintained at 100 kW at nominal voltage. Thus, the variation in active power could be used in parallel, as a measure to detect islanding, with the OVP/UVP and OFP/UFP to decrease the NDZ. Fig. 7 shows the designed islanding detection method for current controlled DGs, where $f_{\max}$, $f_{\min}$, $V_{\max}$, and $V_{\min}$ are the maximum and minimum allowable frequency and voltage respectively. ΔP represents a threshold on the amount of active power deviation. For a value of ΔP equal to 5 kW, the NDZ could be reduced by 50% as compared with the results given in the Appendix. The time delay and ΔP should be chosen accurately in order to avoid nuisance tripping due to disturbances or fluctuations in the voltage level. It should be pointed out that using an active islanding detection method could provide better performance but the paper focuses on passive islanding detection methods.

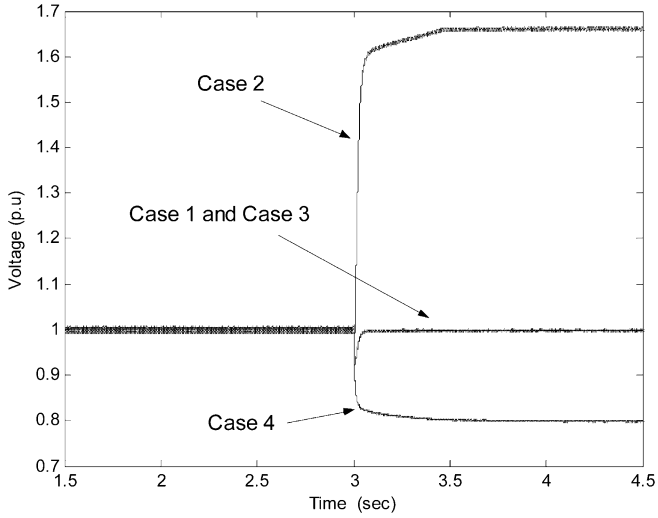

Fig. 6. Voltage at the PCC.

If *((fmax < f < fmin)* ***OR*** *(Vmax < V < Vmin))*
Disconnect DG after a specified time delay
Elseif *100kW+* ΔP ***<*** P_{DG} ***<*** *100 kW -* ΔP
Disconnect DG after a specified time delay
Else
Leave DG operating
End

Fig. 7. Proposed islanding detection method for constant current controlled inverter based DG.

B. Constant P-V Controlled Inverter

This type of interface provides voltage support by injecting reactive power at the PCC. Fig. 8 presents the block diagram of the P-V interface control. Controlling both the active power and voltage to a preset value is not feasible except for two conditions.

1) The DG is connected in parallel with the utility. Any mismatch in power between the load and DG will be delivered/absorbed by the utility.
2) The load resistance satisfies the following condition:

$$R = \frac{3V_{\text{ref}}^2}{P_{\text{ref}}}. \tag{1}$$

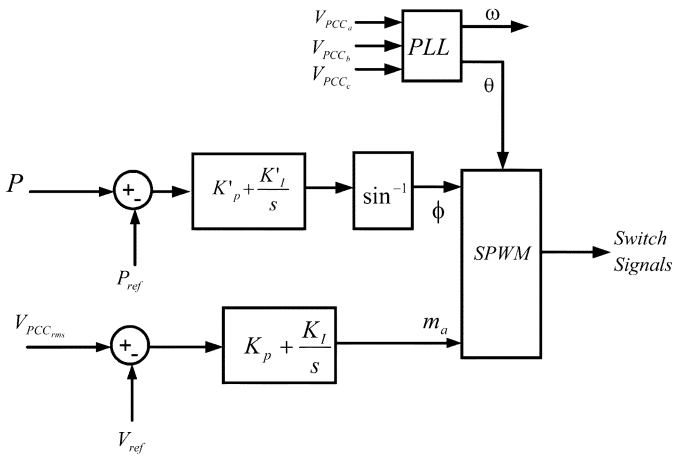

Fig. 8. Power–voltage controlled inverter.

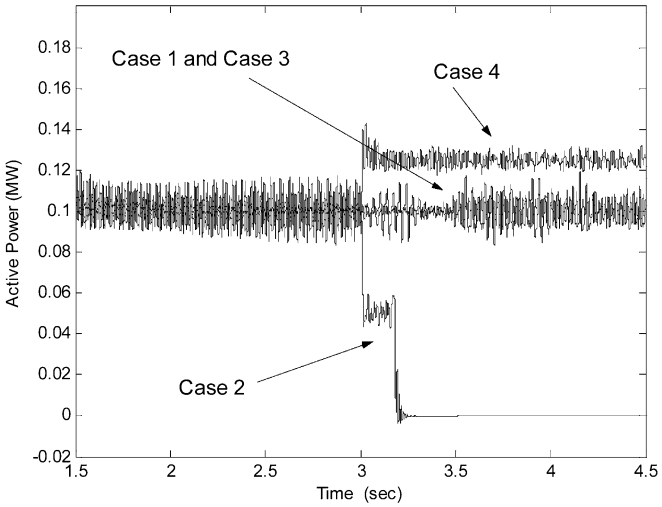

Fig. 9. Active power output of the DG.

If islanding occurs and the load resistance does not equal the resistance calculated in (1), then the DG frequency becomes unstable. Figs. 9–12 present the active power output of the DG, reactive power output of the DG, frequency and voltage at the PCC. It can be seen that the performance of this interface is different from the previous one. Based on the simulation results, for both cases 1 and 3, both the voltage and frequency remain within their standard permissible levels after islanding occurance and islanding will not be detected. This is as a result of the balance between the load and rated DG active power output. Although the load absorbs reactive power (Case 3), the frequency remains at approximately 60 Hz after the DG is islanded due to the capability of this interface of supplying reactive power. For the remaining two cases (Case 2 and Case 4), due to the active power mismatch, the DG becomes unstable and the frequency deviates, thus islanding could be detected using the OVP/UVP and OFP/UFP.

The significant feature for this interface is the frequency at the PCC. The rate of change of frequency (ROCOF) could be used as a parameter for detecting islanding for closely matched active power conditions to reduce the NDZ. Fig. 13 shows the islanding detection algorithm used to detect islanding for P-V controlled inverter based DGs. Similarly, the limits for ROCOF

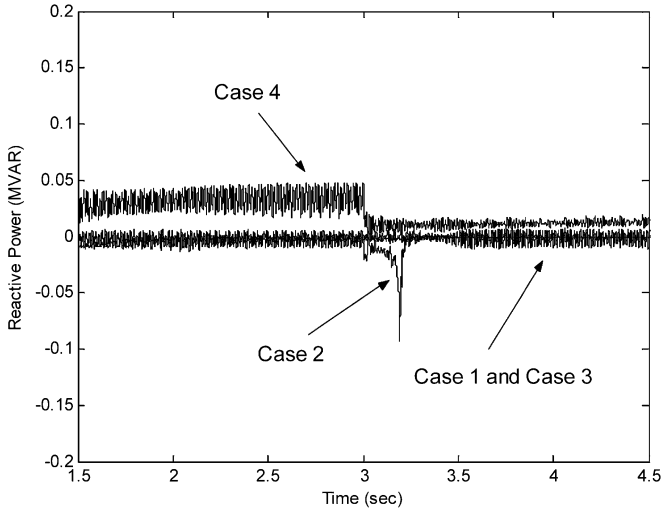

Fig. 10. Reactive power output of the DG.

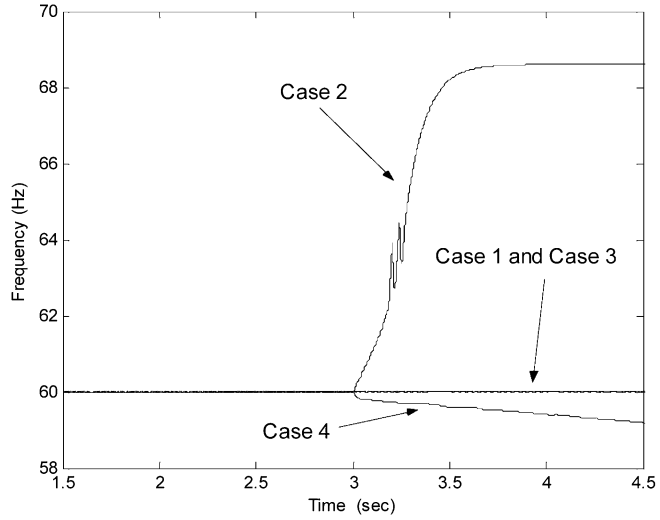

Fig. 11. Frequency at the PCC.

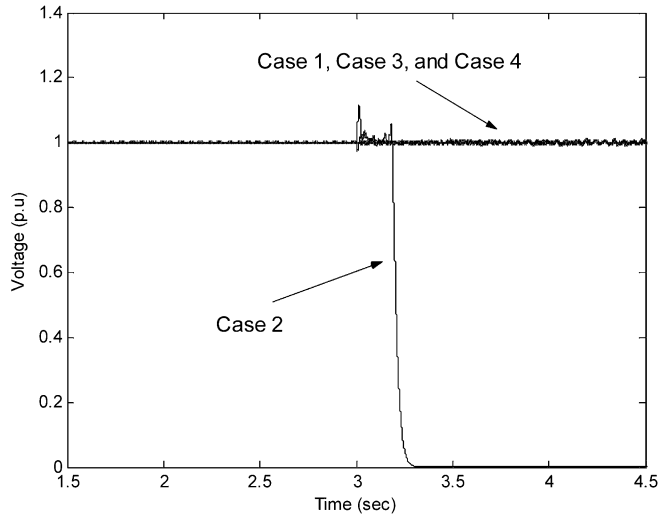

Fig. 12. Voltage at the PCC.

and the time delay are chosen to avoid nuisance tripping. With the ROCOF operating in parallel with the OVP/UVP and

If *((fmax < f < fmin)* ***OR*** *(Vmax < V < Vmin))*
Disconnect DG after a specified time delay
Elseif ROCOFmax < ROCOF < ROCOFmin
Disconnect DG after a specified time delay
Else
Leave DG operating
End

Fig. 13. Proposed islanding detection method for constant P-V controlled inverter-based DG.

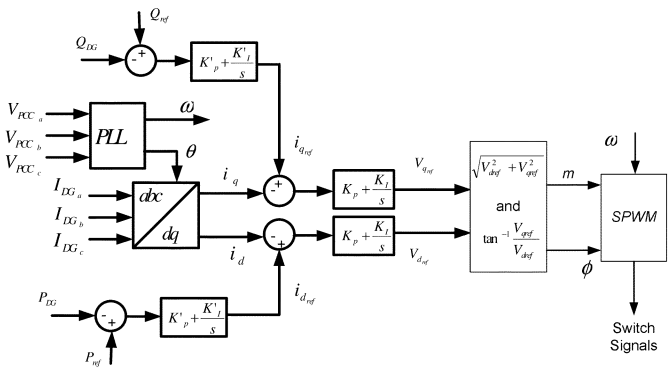

Fig. 14. Block diagram of a PQ controlled inverter.

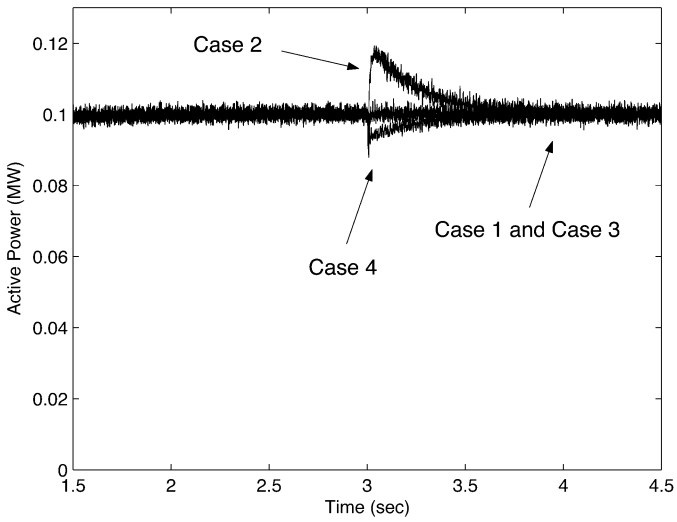

Fig. 15. Active power output of the DG.

OFP/UFP for P-V controlled interfaces, the NDZ becomes very small and thus, implementing an active islanding detection method will not decrease the NDZ of the proposed islanding detection method significantly.

C. Constant P-Q Controlled Inverter

In this case, the active and reactive powers are controlled to a preset value as shown in Fig. 14. Figs. 15–18 present the active power output of the DG, reactive power output of the DG, frequency and voltage at the PCC. The voltage level at the PCC is affected by the active power mismatch while the frequency at the PCC is affected by the reactive power mismatch.

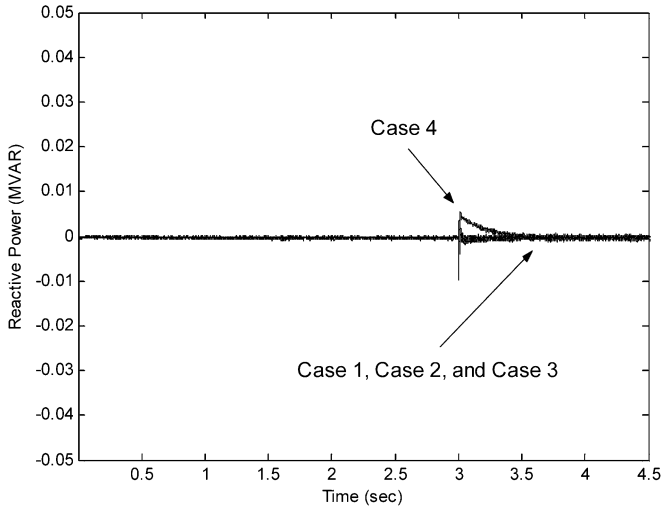

Fig. 16. Reactive power output of the DG.

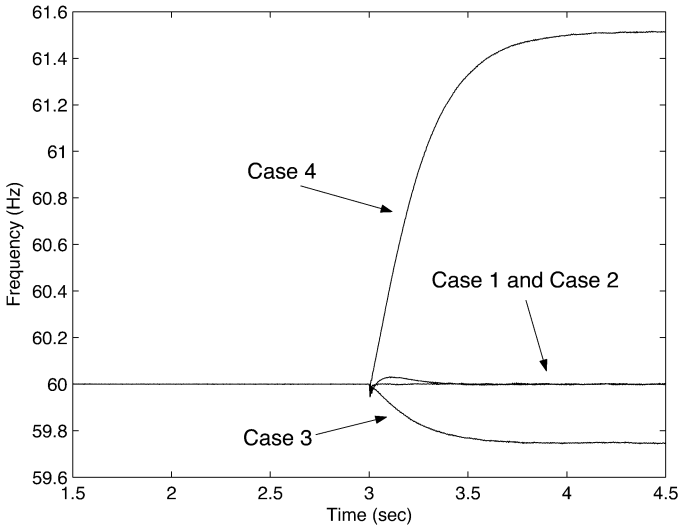

Fig. 17. Frequency at the PCC.

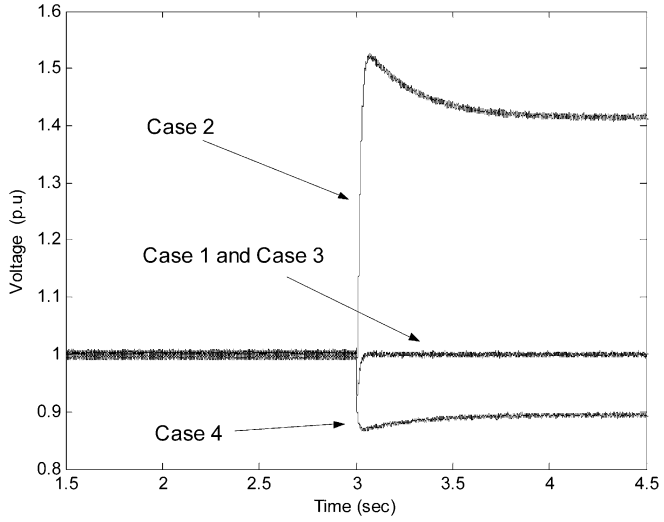

Fig. 18. Voltage at the PCC.

Assuming that the load can be represented as a parallel RLC circuit, these relations can be written in terms of voltage ($V_{\rm PCC}$) and frequency (ω) as follows:

$$P_{\rm load} = \frac{3V_{\rm PCC}^2}{R} \tag{2}$$

$$Q_{\rm load} = 3V_{\rm PCC}^2 \left(\frac{1}{\omega L} - \omega C\right). \tag{3}$$

It can be seen that the value of the PCC voltage is dependent on the island load active power. If the amount of power mismatch is not large enough, the deviation in PCC voltage will not be sufficient to trigger the OVP/UVP. Similarly, for a DG operating at unity power factor, if the load on the island absorbs reactive power, the frequency at the PCC will deviate in order to satisfy the unity power factor operation of the DG. In other words, the frequency will deviate until it reaches the resonance frequency of the load on the island as shown in Fig. 17.

For this interface, both the active and reactive power output of the DG remain fixed, even after islanding occurrence. From the simulation results, the OVP/UVP and OFP/UFP can detect islanding for cases 2 and 4 and will fail to detect for cases 1 and 3. Since, the active power stabilizes at 100 kW even after islanding, thus, the islanding detection algorithm proposed in Fig. 7 will fail for P-Q controlled interfaces. Besides that, the algorithm presented in Fig. 13 using ROCOF can be used to detect islanding. The application of ROCOF for P-Q controlled interfaces will not be as affective as in the case of P-V controlled inverters. This is due to the fact that the P-V interface control becomes unstable during islanding condition. On the other hand, the P-Q interface stabilizes at the resonance frequency once islanding occurs. If the resonance frequency is in close proximity to the 60 Hz value, the ROCOF will fail to detect islanding. Thus, implementing an active islanding detection method could effectively reduce NDZ for the P-Q controlled inverters.

IV. Nondetection Zones

One of the important characteristics to determine the effectiveness of an islanding detection method is the NDZ. NDZ is the operating region where islanding conditions cannot be detected in a timely manner. It can either be represented in terms of power mismatch or in terms of the R, L, and C of the load. In [20], an approximate representation of the NDZ for OVP/UVP was derived. An exact and accurate representation of the NDZ is presented in the Appendix. The paper examines the NDZ of an OVP/UVP and OFP/UVP islanding scheme when implemented for constant current, P-V and P-Q controlled inverters.

For the constant current controlled inverter DG, any change in active power or load resistance will consequently produce a change in the PCC voltage. This is expressed by Ohm's Law as follows:

$$V = IR \tag{4}$$

and thus any small change can be represented by

$$\Delta V = I\Delta R \tag{5}$$

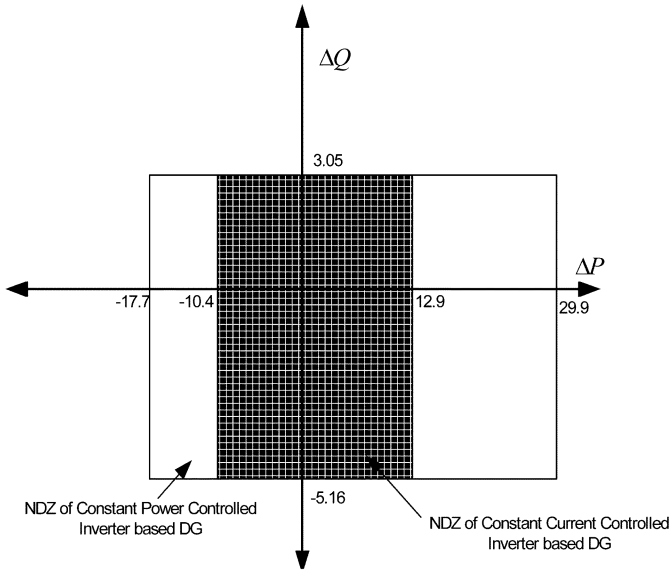

Fig. 19. NDZ for the constant current and constant P-Q interface controls.

where the current I is constant for this type of interface. Since, the reactive power is fixed at zero (unity power factor operation), the frequency will deviate according to the following equation:

$$\omega_r = \frac{1}{\sqrt{LC}}. \tag{6}$$

Despite the fact that constant power controlled inverter based DGs perform the same task as constant current controlled DGs, it was proven by simulations that their response to an islanding situation is different. Similarly, when analyzing the NDZ of constant power DGs, the simulation shows a difference in the NDZ between the two interface controls as shown in Appendix. For an RLC load

$$R = \frac{3V^2}{P}. \tag{7}$$

Since P is constant, then for small changes in R, the change in voltage can be expressed as follows by differentiating (7):

$$\Delta V = \frac{P\Delta R}{6V}. \tag{8}$$

By comparing (5) and (8), it can be seen that for a small change in R, the change in voltage will be different for each type of interface for the same initial loading condition. Thus, the NDZ will differ in both cases. Fig. 19 shows the NDZ of both interfaces determined by simulation. The simulation results match the calculated values given in the Appendix. The results show that the NDZ for constant current controlled inverters is less than $P-Q$ controlled inverters. Thus, the design of the interface control has an effect on NDZ.

Regarding the constant P-V controlled inverter based DGs, there is always a zero reactive power mismatch since the DG is capable of supplying reactive power. Thus, the NDZ of a P-V controlled inverter cannot be illustrated on a ΔP-ΔQ curve. In order to compare this interface with the previous ones, the NDZ was drawn based on the active power and reactive powers of the load. Fig. 20 presents the NDZ of all three interfaces on a P-Q axis reference. Theoretically, there is only one load resistance for which islanding will not be detected as given in (1). Thus,

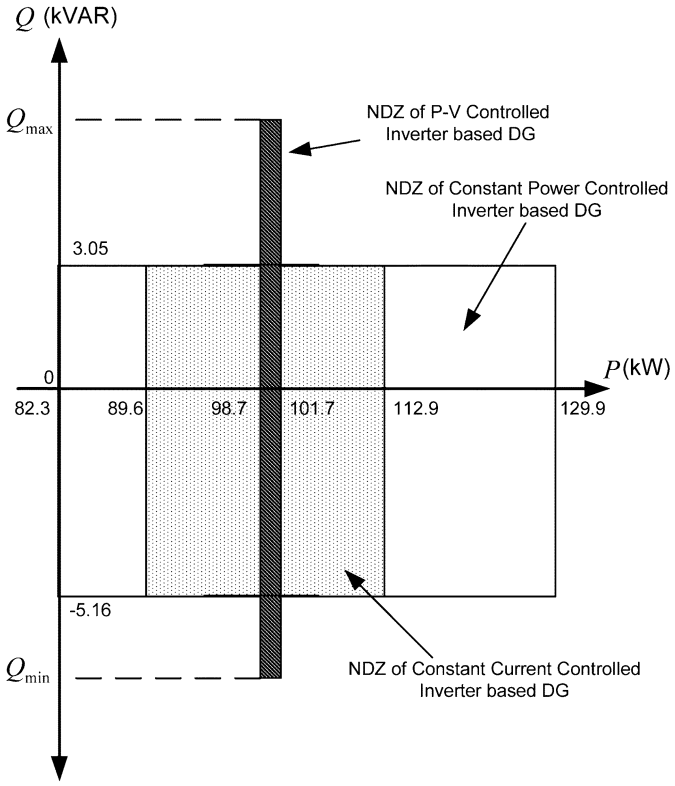

Fig. 20. NDZ for the three interface controls.

for a small amount of active power mismatch, the frequency will deviate and an islanding condition could be detected. On the contrary, since the interface is capable of supplying reactive power, the load reactive power could be as large as the maximum amount of reactive power the DG is capable of supplying. For a small amount of active power mismatch, the frequency will deviate but will reach its threshold value in a large amount of time. Thus, the NDZ for the three interfaces was calculated based on the specified voltage and frequency limits and maximum trip times specified in [10].

TABLE I
SUMMARY OF SIMULATION RESULTS

	Constant Current Controlled	Constant PV Controlled	Constant PQ Controlled
Reference Parameters	d-q component of DG current	Active power and Voltage	Active and reactive power
Case 1	*P*, *Q*, *V*, and *f* remain almost the same	*P*, *Q*, *V*, and *f* remain almost the same	*P*, *Q*, *V*, and *f* remain almost the same
Case 2	*Q*, and *f* remain almost the same but *P* and *V* change	*Q* remains the same but P, *f* and *V* change	*P*, *Q*, and *f* remain almost the same but *V* changes
Case 3	*P*, *Q* and *V* remain almost the same but *f* changes	*P*, *Q*, *V*, and *f* remain almost the same	*P*, *V*, and *Q* remain almost the same but *f* changes
Case 4	*Q* remains almost the same but *P*, *f*, and *V* change	*V* remains almost the same but *P*, *f*, and *Q* change	*P* and *Q* remain almost the same but *f* and *V* change
OVP/UVP an OFP/UFP	Fails to detect islanding for Case 1 and 3	Fails to detect islanding for Case 1 and 3	Fails to detect islanding for Case 1 and 3
NDZ using OVP/UVP an OFP/UFP	Large but almost 50% less than Constant Power DG	Small but takes large operating time for close to rated power loading conditions	Largest
Passive method for NDZ Reduction	Using Active Power in parallel with OVP/UVP and OFP/UFP	Using ROCOF ratio in parallel with OVP/UVP and OFP/UFP	Active Power fails in islanding detection. ROCOF could be used

V. DISCUSSION

Prior to concluding the results presented in this paper, the scope of this study must be reclarified. The paper studies the impact of DG interface control on islanding detection in general and on the NDZ of the OVP/UVP and OFP/UFP. The study does not include the impact of interface control on active islanding detection methods and other passive islanding detection methods. The paper outlines certain types of interface controls and not all for brevity purposes. The purpose of the presented islanding detection methods is to highlight the effect of the interface control on the choice of an islanding detection method and not to enhance the performance of currently proposed islanding detection methods in previous work. Furthermore, for constant current and P-Q controlled inverters capable of injecting reactive power, islanding detection becomes much more complicated since there will be no reactive power mismatch during an islanding condition that will lead to a frequency deviation. This could have an impact on islanding detection methods that depend on reactive power mismatch and frequency deviation. Several issues, which require further investigation:

1) effect of interface control on other islanding detection methods.
2) impact of reactive power injection on NDZ and islanding detection methods dependent on reactive power variation.

A summary of the simulations results is given in Table I.

VI. CONCLUSION

This paper studied the impact of DG interface control on islanding detection and NDZ of OVP/UVP and OFP/UFP. Constant current, constant P-V, and constant P-Q interface controls were analyzed and the following conclusions were drawn.

1) Each interface responds differently to an islanding situation. Thus, an islanding detection algorithm can work efficiently for certain types of DG interface control and inefficiently for other types.
2) For DGs operating at unity power factor, constant current controlled inverters are advantageous over constant P-Q controlled inverters due to their small NDZ.
3) The derived NDZ for OVP/UVP and OFP/UFP are more accurate and provide better representation of the NDZ.
4) For DGs capable of supplying reactive power, as in the case of the constant P-V controlled DG, the NDZ cannot be represented on a ΔP-ΔQ curve. In this case, the NDZ is better represented on a P-Q curve.
5) Detecting an islanding situation for constant P-V controlled interfaces is easier than the other interfaces presented in this paper.
6) Instead of designing a sophisticated islanding detection algorithm to decrease the NDZ, implementing a suitable control strategy that inherently has a small NDZ can significantly reduce the complexity of the islanding detection algorithm.

The results and conclusions prove that DG interface control has an impact on islanding detection and NDZ.

APPENDIX

A. Constant Current Controlled DGs

In order to determine the amount of mismatch for which the OVP/UVP and OFP/UFP will fail to detect islanding, the amount of active power mismatch in terms of load resistance can be expressed as follows:

$$\Delta P = 3V \cdot I - 3(V \pm \Delta V \cdot V) \cdot I = \pm 3V \cdot \Delta V \cdot I. \quad (9)$$

For a voltage ranging from 88% to 110%, the amount of power mismatch calculated using (9) equals 12 kW and 10 kW respectively. In [20], a mathematical formula for reactive power mismatch was presented. Unfortunately the equation derived involved approximation. A simple and accurate derivation for determining the NDZ is presented. The load reactive power can be expressed as follows:

$$Q_{\text{load}} = 3V^2 \left(\frac{1}{\omega_n L} - \omega_n C \right). \quad (10)$$

Since the DG is operated at unity power factor, the amount of reactive power mismatch is equal to the load reactive power and can be expressed as follows:

$$\Delta Q = \frac{3V^2}{\omega_n L} \left(1 - \omega_n^2 LC\right) = \frac{3V^2}{\omega_n L} \left(1 - \frac{\omega_n^2}{\omega_r^2}\right). \quad (11)$$

The resonance frequency can be expressed in terms of the nominal frequency and the frequency variation as follows:

$$\omega_r = \omega_n \pm \Delta\omega \quad (12)$$

and (11) can be written in terms of the frequency variation as follows:

$$\Delta Q = \frac{3V^2}{\omega_n L} \left(1 - \frac{f_n^2}{(f_n \pm \Delta f)^2}\right) \quad (13)$$

TABLE II
SYSTEM PARAMETERS

Inverter		
Switching frequency		8000 Hz
Input DC voltage		900 V
Filter Inductance		2.1 mH
Voltage (Line to Line)		480 V
DG Output Power		100 kW
Load Parameters		
R		2.304
L		3.395 mH
C		2.075 mF
Grid Parameters		
Frequency		60 Hz
Grid inductance		0.3056 mH
Grid resistance		0.012 Ω
Controller parameters		
I_d-I_q	$K_I = 0.01$	$K_p = 20$
P-V	$K_I = 0.08$, $K'_I = 0.008$	$K_p = 0.1$, $K'_p = 0.1$
P-Q	$K_I = 0.0008$, $K'_I = 0.1$	$K_p = 2.5$, $K'_p = 20$

where ω_n and ω_r are the nominal and resonance frequency. L and C are the load inductance and capacitance. The values of reactive power mismatch for a frequency threshold ranging from 59.3 Hz to 60.5 are 5.1 and 3.074 KVAR, respectively. The results determined in (13) provide accurate results as compared with the results presented in [20].

B. Constant P-Q Controlled DGs

Similarly, an equation for the active power mismatch was derived in [20]. A simple derivation is presented and provides the same results presented in [20]. Since the active power output of the DG is constant, the value of load resistance that will produce a sufficient change in voltage that could be detected by the islanding protection can be calculated from the following expression:

$$\frac{3((1 \pm \Delta V)V)^2}{R_2} = \frac{3V^2}{R_1} \quad (14)$$

$$R_2 = R_1(1 \pm \Delta V)^2 \quad (15)$$

where R_1 represents the value of load resistance that absorbs the rated DG active power. R_2 represents the value of load resistance that will cause a deviation in voltage equal to ΔV.

The active power mismatch in this case is the difference between the active power absorbed by R_1 and R_2 and can be expressed as follows:

$$\Delta P = \frac{3V^2}{R_1} \left(1 - \frac{1}{(1 \pm \Delta V)^2}\right). \quad (16)$$

For a voltage ranging from 88% to 110%, the amount of power mismatch calculated using (16) equals 29.3 kW and 17.3 kW, respectively. Similarly, the amount of reactive power mismatch can be calculated from (13). The system, controller and load parameters are given in Table II.

REFERENCES

[1] Y. Xue, L. Chang, S. B. Kjaer, J. Borddonau, and T. Shimizu, "Topologies of single phase inverters for small distributed power generators: An overview," *IEEE Trans. Power Electron.*, vol. 19, no. 5, pp. 1305–1313, Sep. 2004.
[2] *IEEE Standard for Interconnecting Distributed Resources With Electric Power Systems*, IEEE Std. 1547-2003, 2003.

[3] P. G. Barbosa, L. G. Rolim, E. H. Watanabe, and R. Hanitsch, "Control strategy for grid-connected DC-AC converters with load power factor correction," *Proc. Inst. Elect. Eng., Gen., Transm. Distrib.*, vol. 145, no. 5, pp. 487–491, Sep. 1998.
[4] S. Huang and F. Pai, "Design and operation of grid-connected photovoltaic system with power-factor control and active islanding detection," *Proc. Inst. Elect. Eng., Gen., Transm. Distrib.*, vol. 148, no. 2, pp. 243–250, Mar. 2001.
[5] M. I. Marie, E. F. El-Saadany, and M. M. A. Salama, "Flexible distributed generation: (FDG)," in *Proc. IEEE Power Eng. Soc. Meeting*, vol. 1, Jul. 2002, pp. 49–53.
[6] M. A. Kashem and G. Ledwich, "Distributed generation as voltage support for single wire earth return systems," *IEEE Trans. Power Del.*, vol. 19, no. 3, pp. 1002–1011, Jul. 2004.
[7] M. Marie, E. F. El-Saadany, and M. M. A. Salama, "A novel control algorithm for the DG interface to mitigate power quality problems," *IEEE Trans. Power Del.*, vol. 19, no. 3, pp. 1384–1392, Jul. 2004.
[8] S. Barsali, M. Ceraolo, P. Pelacchi, and D. Poli, "Control techniques of dispersed generators to improve the continuity of electricity supply," in *Proc. IEEE Power Eng. Soc. Winter Meeting*, vol. 2, Jan. 2002, pp. 789–794.
[9] S. Park, I.-Y. Chung, and Joon-Ho, "Control schemes of the inverter-interfaced multi-functional dispersed generation," in *Proc. IEEE Power Eng. Soc. General Meeting*, vol. 3, Jul. 2003, pp. 1924–1929.
[10] "Static Inverter and Charge Controllers for Use in Photovoltaic Systems," Underwriters Laboratories Inc., Northbrook, IL, UL 1741, Std. 1741.
[11] G. Kern, "Sunsine300, utility interactive AC module anti islanding test results," in *Proc. IEEE Photovoltaic Specialist Conf.*, Sep. 1997, pp. 1265–1268.
[12] M. Redfern, O. Usta, and G. Fielding, "Protection against loss of utility grid supply for a dispersed storage and generation unit," *IEEE Trans. Power Del.*, vol. 8, no. 3, pp. 948–954, Jul. 1993.
[13] F. Pai and S. Huang, "A detection algorithm for islanding prevention of dispersed consumer owned storage and generating units," *IEEE Trans. Energy Convers.*, vol. 16, no. 4, pp. 346–351, Dec. 2001.
[14] M. Ropp and W. Bower, "Evaluation of Islanding Detection Methods for Photovoltaic Utility Interactive Power Systems," International Energy Agency Implementing agreement on Photovoltaic Power Systems, Tech. Rep. IEA PVPS T5-09, 2002.
[15] S. Salman, D. King, and G. Weller, "New loss of mains detection algorithm for embedded generation using rate of change of voltage and change in power factor," *Proc. Inst. Elect. Eng. Development in Power System Protection*, pp. 82–85, Apr. 2001.
[16] S. Jang and K. Kim, "An islanding detection method for distributed generations using voltage unbalance and total harmonic distortion of current," *IEEE Trans. Power Del.*, vol. 19, no. 2, pp. 745–752, Apr. 2004.
[17] C. Jeraputra, P. Enjeti, and I. Hwang, "Development of a robust anti-islanding algorithm for utility interconnection of distributed fuel cell powered generation," in *Proc. IEEE Appl. Power Electron. Conf. Expo.*, vol. 3, Feb. 2004, pp. 1534–1540.
[18] T. C. Wang, Z. Ye, G. Sinha, and X. Yuan, "Output filter design for a grid interconnected three phase inverter," in *Proc. IEEE 34th Annu. Power Electronics Specialist Conf.*, vol. 2, Jun. 2003, pp. 779–784.
[19] Z. Ye, R. Walling, L. Garces, R. Zhou, L. Li, and T. Wang, "Study and Development of Anti-Islanding Control for Grid-Connected Inverters," General Electric Global Research Center, NREL/SR-560-36 243, 2004.
[20] Z. Ye, A. Kolwalkar, Y. Zhang, P. Du, and R. Walling, "Evaluation of anti-islanding schemes based on nondetection zone concept," *IEEE Trans. Power Electron.*, vol. 19, no. 5, pp. 1171–1176, Sep. 2004.

H. H. Zeineldin (M'05) received the B.Sc. and M.Sc. degrees in electrical engineering from Cairo University, Cairo, Egypt, in 1999 and 2002, respectively. He is currently pursuing the Ph.D. degree in electrical and computer engineering at the University of Waterloo, Waterloo, ON, Canada.

His interests include protective relay coordination and distributed generators.

Ehab F. El-Saadany (SM'05) was born in Cairo, Egypt, in 1964. He received the B.Sc. and M.Sc. degrees in electrical engineering from Ain Shams University, Cairo, Egypt, in 1986 and 1990, respectively, and the Ph.D. degree in electrical engineering from the University of Waterloo, Waterloo, ON, Canada, in 1998.

Currently, he is an Associate Professor in the Department of Electrical and Computer Engineering, University of Waterloo. His research interests are distribution system control and operation, power quality, power electronics, digital signal processing (DSP) applications to power systems, and mechatronics.

M. M. A. Salama (F'02) received the B.Sc. and M.Sc. degrees in electrical engineering from Cairo University, Cairo, Egypt, in 1971 and 1973, respectively, and the Ph.D. degree in electrical engineering from the University of Waterloo, Waterloo, ON, Canada, in 1977.

Currently, he is a Professor in the Department of Electrical and Computer Engineering, University of Waterloo. His interests include the operation and control of distribution systems, cables, insulation systems, power-quality monitoring and mitigation, and electromagnetics. He has consulted widely with government agencies and the electrical industry. He is a registered Professional Engineer in the Province of Ontario.